

Ultra-high fuel utilization in polymer electrolyte fuel cells part I: An experimental study

X.G. Yang, Y. Wang & C.Y. Wang

To cite this article: X.G. Yang, Y. Wang & C.Y. Wang (2021): Ultra-high fuel utilization in polymer electrolyte fuel cells part I: An experimental study, International Journal of Green Energy, DOI: [10.1080/15435075.2021.1941041](https://doi.org/10.1080/15435075.2021.1941041)

To link to this article: <https://doi.org/10.1080/15435075.2021.1941041>



Published online: 07 Jul 2021.



Submit your article to this journal [↗](#)




View related articles [↗](#)



View Crossmark data [↗](#)



Ultra-high fuel utilization in polymer electrolyte fuel cells part I: An experimental study

X.G. Yang, Y. Wang, and C.Y. Wang 

Electrochemical Engine Center, and Department of Mechanical and Nuclear Engineering, The Pennsylvania State University, University Park, PA, USA

ABSTRACT

In this study, a high fuel utilization approach for polymer electrolyte fuel cells (PEFC) is proposed and studied experimentally. This approach uses an ultra-low hydrogen stoichiometry supply (i.e., $\xi_a = 1.02$) meanwhile sustaining stable cell performance. Systematic experiments showed the feasibility of high fuel utilization approach under different pressures and hydrogen/air inlet humidification conditions. It is indicated that the fuel cell is able to provide stable performance at a real fuel stoichiometry $\xi_a = 1.02$ under high-current density operation. For all the tests at $\xi_a/\xi_c = 1.5/2.0$ or $1.02/2.0$, there exist unstable operation regimes typically in low power conditions. The instability as a result of flooding is affected mainly by air stoichiometry and less by fuel stoichiometry.

ARTICLE HISTORY

Received 3 February 2021
Accepted 26 April 2021

KEYWORDS

Fuel utilization; low stoichiometry; operation stability; water management; hydrogen; fuel cells

1. Introduction

Tremendous progress on key technologies has been achieved, allowing polymer electrolyte fuel cells (PEFC) to provide higher power densities and more operational flexibility than ever before. Most cell performance data published to date have been evaluated with large stoichiometries, or excessive reactant gases. The reason for using high stoichiometries is to keep research objectives free from the negative effect of potential mass transport limitation. The stoichiometries of hydrogen and air supplies in the literature are usually in the range of 1.2 – 2.0 and 2.0–4.0, respectively (O'hayre et al. 2016; Wang, Basu, and Chao-Yang Wang 2008). It means that, taking hydrogen as an example, 20–100% more hydrogen fuel is introduced into the cell and then exits as exhaust without electrochemical reactions. From point of view of energy efficiency and safety issue, such an approach with large fuel stoichiometries is definitely unacceptable for engineering applications, and thus effective methods of fuel feeding shall be found.

Re-circulating excess hydrogen by using an ejector can improve fuel efficiency in PEFCs (Du Plooy, Meyer, and von Solms 2018; Jiang et al. 2017; Rabbani and Rokni 2013). The system for fuel re-circulation is sort of a dead-end configuration (Manokaran et al. 2011). If without effective water removal (Grimm et al. 2020; Voss et al. 1995; Xing et al. 2016) water accumulation in dead-end flow fields is prone to causing cell flooding and parasitic effects on cell health, e.g., poisonous substances depositing on catalysts, electrode microstructure changes, and over-swollen polymer membranes. Being aware of these potential threats, the authors in Ref Berg et al. (2004) attempted to expel water out of fuel stream by means of pressure waves, generated by pumping periodical high-

pressure pulses of stream into the cell or creating vacuum-pressure pulses at the outlet to suck hydrogen out of the cell. The impact from pressure waves on the durability of thin membranes is expected not to be slight, but have not been assessed yet (Ichikawa et al. 2014). One obvious disadvantage of recirculation arrangement is the introduction of complex flow control algorithms and burdens of extra auxiliary systems. Comparison of different anodic recirculation systems was studied by Toghyani et al. (Toghyani, Baniasadi, and Afshari 2018; Toghyani, Afshari, and Baniasadi 2019).

It is ideal to feed a PEFC with the same amount of hydrogen exactly as that consumed by electrochemical reaction at any current densities, or at a real stoichiometry of 1.0. In this case, no hydrogen remains in the anode exhaust except water if pure hydrogen gas is used as the fuel. Due to consumption of humidified hydrogen, water vapor in the fuel stream becomes concentrated probably to condensate in anode channels, and cause flooding, too. As a consequence, fuel starvation occurs downstream in channels clogged by liquid water, leading to lower cell voltages and unstable cell performance. In a worse case when the flooded cell is working in a stack in serial, fuel starvation will lead to a breakdown of electrochemical reactions by a rapid drop cell voltage.

Engineering questions arise on how low-fuel stoichiometries can be without obvious performance loss, and what negative effects on cells can be. Unfortunately, there is very limited information available in the literature to the questions. This paper focused on this topic and discussed the effects of ultra-low hydrogen stoichiometry on cell performance and stability at various loads and operation conditions. In addition, comparing with the dead-end configuration, a cell with ultra-low hydrogen stoichiometry supply has an anode outlet, permitting the very little unused hydrogen to flow out. Because only little

unused hydrogen, there is no need for fuel recirculation system, which is beneficial to system control, design, and cost reduction. Experimental results indicated that the cell could run steadily with no sign of performance loss under an ultra-low fuel stoichiometry. In a companion paper (Part 2), numerical simulation was conducted to explain the experimental observations and support our hypothesis.

2. Experimental

Tests were conducted in an in-house designed single-cell fixture using membrane-electrode-assemblies (MEAs) with a 30 μm thick composite membrane (Equivalent molar weight < 1000). Catalyst loading at each side of electrode was 0.4 mg-Pt/cm². The gas diffusion media is wetproof carbon cloth with a microporous layer facing the catalyst electrode. Microporous layers are proven necessary to help expel water out of the active sites effectively, but the mechanism by which water transports from the catalyst layer into the gas diffusion layer (GDL) is unclear. Both anode and cathode flow fields are identical, composed of seven parallel straight gas channels. Each gas channel is 1 mm wide, 1 mm deep, and 100 mm long. Six current landing ridges (1 mm wide each) evenly separate seven gas channels. Therefore, the cell has a total active area of 14 \times 100 mm². Table 1 lists the fuel cell geometrical and operating parameters.

In this study, pure hydrogen and air were used in a co-flow configuration. Two sets of stoichiometries were chosen: one set of real stoichiometries was 1.5/2.0 (H₂/air); the other was 1.02/2.0. All tests had the same air flow condition ($\xi_a = 2.0$), so that the effect of ultra-low fuel stoichiometry can be isolated from other factors.

Experimental results at different conditions will provide us with more information for the understanding of the mechanisms. Two operation pressures and different inlet humidification were also chosen for comparison studies. Cell pressures were adjusted by setting the backpressure at 2 or 1 atm (absolute). Both anode and cathode pressures were always the same in one test. Cell temperature was set at 80°C. Tests with inlet fuel/air dew point of 80°C were conducted first, and then another set of tests with reduced air inlet humidification (50% relative humidity) followed. All test parameters can be

Table 1. Geometrical and operating parameters.

Quantity	Value
Gas flow channel depth/ width	1.0/1.0 mm
Gas flow channel length	100.0 mm
Gas flow channel pattern	7 parallel straight
Shoulder width	1.0 mm
Membrane (WL Gore®) thickness	0.03 mm
MEA active area	1400 mm ²
Catalyst loading at each side	0.4 mg-Pt/cm ²
GDL	Wetproof carbon cloth
Anode/cathode inlet pressures	2.0/2.0 atm
Cathode stoichiometry (real-stoichiometric test)	2.0
Anode stoichiometry (real-stoichiometric test)	1.02 or 1.5
Anode/cathode stoichiometry (fixed-flow-rate test)	1.5/2.0 @ 1.0 A/cm ²
Temperature of fuel cell, T	353.15 K
Relative humidification of anode injection	100%
Relative humidification of cathode injection	100% or 50%

computer-controlled by a fuel cell test station (Arbin Instruments, TX) with its commercial software MIT'S Pro.

We conducted all tests under a constant current mode, so flow rates of reactant gases can be controlled according to specified stoichiometries at a given current density (or in real-stoichiometry-controlled mode). Otherwise, gas flow rates have to be adjusted to cope with real-time currents, if tests were conducted under a constant voltage mode. Cell voltages were determined by averaging voltage readings in the last minute for each step of constant current tests.

We found that under real-stoichiometry-controlled mode, the cell operation became unstable when flow rates of reactant gases (or currents) were less than a threshold value. Further, we found that cell performance instability was due to insufficient airflows in the low-current regime. In order to get full spectra of polarization, a minimum airflow rate was fixed for tests in the low-current regime, while fuel flow rates still varied with currents according to a specified stoichiometry.

In comparison with real stoichiometric tests, fixed-flow-rate tests were also conducted at a flow rate of 0.146/0.464 (H₂/air) standard liters per minute (slpm), or at a stoichiometry of 1.5/2.0, referenced to 1.0 A/cm². It meant that the flow rates are constant at any current densities. Performance comparison between real-stoichiometric tests and fixed-flow-rate tests in the same paper is necessary, since some performance data in the literature were obtained in a fixed-flow-rate control mode (Berg et al. 2004; Chakraborty 2019; O'hayre et al. 2016).

3. Results and discussion

3.1. Effect of fuel stoichiometry

3.1.1. Tests at 2 atm and real stoichiometry $\xi_a/\xi_c = 1.5/2.0$

Tests under 2 atm absolute and real stoichiometry of $\xi_a/\xi_c = 1.5/2.0$ are the baseline case. Reactant gases were fully humidified before entering the cell. Tests started with a constant current of 1.0 A/cm². Fuel/air flow rates were set constantly at 0.146 and 0.464 slpm, respectively, according to the specified stoichiometry $\xi_a/\xi_c = 1.5/2.0$. In this case, the cell voltage became stable at 0.602 V within 5 minutes after polarizing. Then the current increased by an interval (e.g., 50 mA/cm²), and flow rates increased according to $\xi_a/\xi_c = 1.5/2.0$. The software coming with the test station is able to reset flow rates automatically. Another steady voltage was read after polarization was stable. Repeating these cycling steps till the cell current reached 1.4 A/cm². Typical cell performances are represented by: 0.602 V at 1 A/cm² and 0.482 V at 1.4 A/cm² without IR correction. After finishing high-current tests, we continued to test in the low-current regime starting from 0.9 A/cm² down to 0.1 A/cm², and the steady voltage was thus recorded in each step. Figure 1 shows the current-voltage (*I*-*V*) polarization measured at 2 atm with a real stoichiometry of $\xi_a/\xi_c = 1.5/2.0$. The nearly linear plot indicates that the cell performance is dominated by electrochemical kinetics, without obvious sign of mass transport limitation at 1.4 A/cm².

The cell operated steadily under a real stoichiometry of $\xi_a/\xi_c = 1.5/2.0$ until the current was lower than 0.3 A/cm² (0.782 V). Unstable cell performance was symbolized by vigorous voltage fluctuation, which will be discussed later.

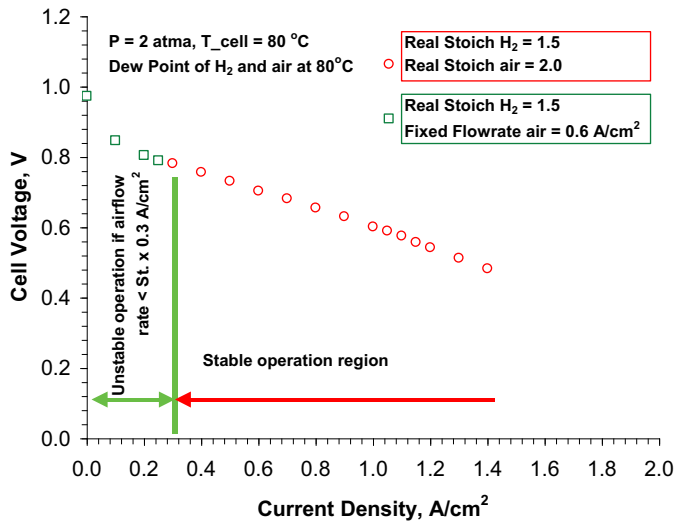


Figure 1. I–V polarization curve under real stoichiometry control: $\xi_a = 1.5$, $\xi_c = 2.0$ times real current density, and 2 atm.

By adjusting fuel or air flow rate separately, we found the cause for performance instability in the region $I < 0.3 \text{ A/cm}^2$ is that the stoichiometric airflow rates were not sufficient. Increasing airflow rates up to a certain level avoids operation instability. This is due to the fact that insufficient stoichiometric airflow rates cannot efficiently remove liquid water produced by fuel cells, leading to unstable operation. Similar phenomenon was observed in Ref. Wang, Basu, and Chao-Yang Wang (2008). On the other hand, the cell was unable to sustain steady voltages if only raising fuel stoichiometry to a higher level (i.e., $\xi_a = 5$) while maintaining air stoichiometry at 2.0 unchanged. Therefore, a fixed airflow at a rate equivalent to 0.6 A/cm^2 (or air stoichiometry $\xi_{air} \times 0.3 \text{ A/cm}^2$) was employed, and hydrogen flow rates were still adjusted according to $\xi_a = 1.5$, polarization tests in this region ($I < 0.3 \text{ A/cm}^2$) were completed and its I–V plot was included in Figure 1.

3.1.2. Tests at 2 atm and $\xi_a/\xi_c = 1.02/2.0$

In the following, we investigated the effect of a reduced anodic stoichiometry ($\xi_a = 1.02$) on cell performance, with otherwise identical test parameters. Applying the same methodology as used above, the polarization curve under the ultra-low ξ_a condition was obtained and given in Figure 2. One obvious effect of reducing ξ_a from 1.5 to 1.02 is to expand the instability operation regime, with an increase in threshold current density from previous 0.3 to 0.7 A/cm^2 . Similarly, a fixed airflow (equivalent to 2.0 A/cm^2) and stoichiometric fuel gas feeding were used to test the I–V polarization in the region $I < 0.7 \text{ A/cm}^2$; and the entire polarization test was completed as shown in Figure 2.

In order to show clearly the effect of fuel stoichiometry, both results under $\xi_a = 1.02$ and 1.5 are compared and summarized in Figure 3. The combined figure shows no loss in cell performance in the range of 0.7 – 1.4 A/cm^2 as the fuel stoichiometry decreases from 1.5 to 1.02 . Interestingly, cell voltages around 1.0 A/cm^2 become slightly higher at $\xi_a = 1.02$ than at 1.5 , probably due to the MEA humidified better under a lower

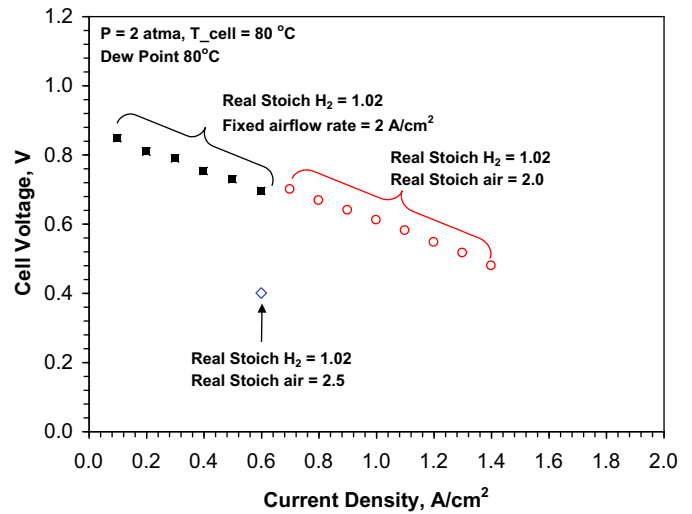


Figure 2. I–V polarization curve: high-current density region under real stoichiometry control: $\xi_a = 1.02$, $\xi_c = 2.0$ times of real current density; and low-current density region with fixed airflow rate at 2 A/cm^2 or 2.0 stoichiometry at 1 A/cm^2 , and real stoichiometry control: $\xi_a = 1.02$. The reason to use fixed airflow rate at low-current region is to obtain stable cell operation.

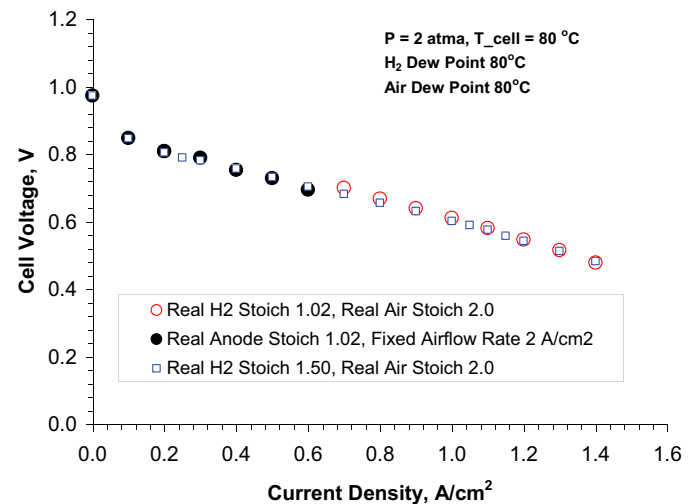


Figure 3. Comparison between normal (1.5) and ultra-low (1.02) real anode stoichiometry. Test conditions are the same as in Figures 1 and Figures 2. For the fixed airflow rate of 2 A/cm^2 , the stoichiometry is 2.0 at 1 A/cm^2 .

fuel flow rate (Wang, Basu, and Chao-Yang Wang 2008) or experimental uncertainty.

Unstable cell operation was represented by vigorous voltage fluctuations in low-current regime. Figures 4 and Figures 5 show the cell voltage versus test time after the cell was polarized ($\xi_a = 1.02$) at current density of 1.0 and 0.6 A/cm^2 , respectively. Other test conditions were identical with that in Figure 2. The stable cell voltages as shown in Figure 4 were recorded at 1.0 A/cm^2 , slightly dropping from initial 0.623 V to 0.614 V in 22 min after polarization, indicating minor flooding at the cathode. In contrast, the cell voltage at a current density of 0.6 A/cm^2 decreased gradually in the first minute starting from 0.726 V , and then became oscillating aggressively in a range of 0.72 – 0 V . Occasionally, a negative voltage was read. As we mentioned above, performance instability was directly related to

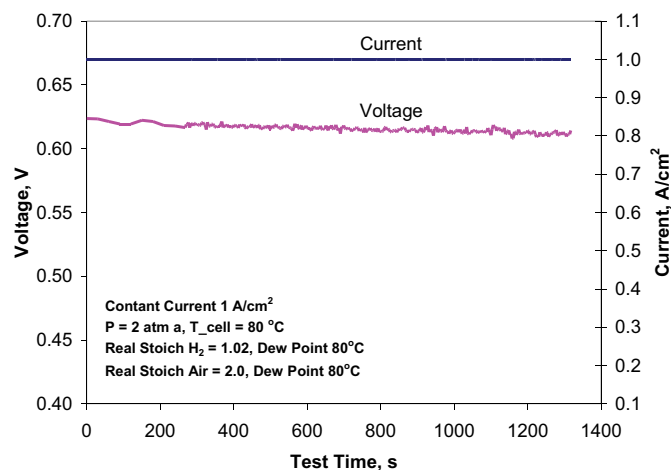


Figure 4. Stable cell voltage versus time under constant current density of 1.0 A/cm² at ultra-low anode real stoichiometry ($\xi_a = 1.02$) and normal air real stoichiometry of ($\xi_c = 2.0$) in a 14 cm² cell.

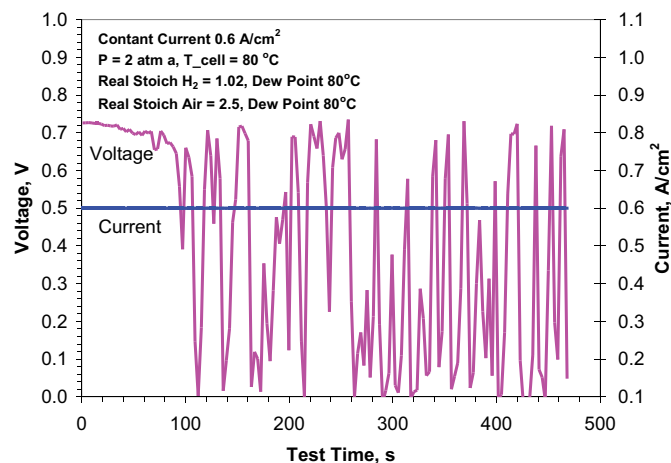


Figure 5. Cell voltage fluctuation versus time under constant current density of 0.6 A/cm² at ultra-low anode real stoichiometry ($\xi_a = 1.02$) and normal air real stoichiometry of ($\xi_c = 2.0$) in a 14 cm² cell.

insufficient airflow rates, not as a result of fuel starvation either at $\xi_a = 1.02$ or 1.5. To further verify this, an additional test at 0.6 A/cm² with a greater air stoichiometry of 2.5 showed an average cell voltage of 0.4 V, as indicated by the sporadic dot in Figure 2. In this case, voltage fluctuation still existed, but the amplitude of voltage fluctuation decreased; and the cell voltage stayed in a relatively high value in most of the time. Further increasing air stoichiometry eventually mitigated the voltage fluctuation (data not shown in the figure). It is clear that high fuel utilization approach is associated with flooding not only in the anode but also the cathode.

3.2. Effect of operation pressures

Generally, a reduced operation pressure results in a lower cell performance. On the other hand, reduced pressures increase velocities of reactant gas streams given at the same stoichiometries and cell temperatures. Thus, a reduced operation pressure will alleviate the flooding problem in the cell to some

extent, thus it may be interesting to see the effect of gas pressures under high fuel utilization operations.

3.2.1. Tests at 1 atm and $\xi_a/\xi_c = 1.5/2.0$

Figure 6 shows the polarization performance under conditions of 1 atm absolute and real stoichiometry of $\xi_a/\xi_c = 1.5/2.0$. The cell voltage at 1.0 A/cm² was 0.490 V; there is a penalty of 0.112 V due to pressure drop from 2 to 1 atm. In the lower voltage region (< 0.45 V), another controlling mechanism that may be transportation limitation kicked in as indicated by the deviation in I - V curve. The maximum current density reached 1.1 A/cm² at 0.363 V.

One can see that the threshold current density for unstable operation was still 0.3 A/cm², the same as at 2 atm (Figure 1). When the current density was less than 0.3 A/cm², a fixed airflow rate (0.6 A/cm²) and a stoichiometric hydrogen flow rate were used to complete the rest of tests.

3.2.2. Test at 1 atm and $\xi_a/\xi_c = 1.02/2.0$

Cell performance under ultra-low stoichiometry fuel supply and 1 atm was also systematically investigated, as shown in Figure 7. In this case, the threshold current density was 0.6 A/cm², close to 0.7 A/cm² at 2 atm (Figure 2). With a reduced $\xi_a = 1.02$, the cell was still able to generate a current density of 1.1 A/cm², the same as that with $\xi_a = 1.5$ (Figure 6), but at a higher voltage of 0.419 V. By setting airflow rate at 2.0 A/cm² equivalent and stoichiometrically adjusting the fuel flow rate, polarization tests in the range of 0.1–0.5 A/cm² were finished and plotted in Figure 7. It demonstrated again that steady cell operation is achievable even under a hydrogen stoichiometry as low as 1.02, providing that the airflow rate is sufficient.

In order to clearly show how airflow rates are related to cell operation stability, another set of tests was conducted with various airflow rates at the same current density of 0.5 A/cm², under conditions: hydrogen flow rate was fixed at 1.02×0.5 A/cm² equivalent, and the airflow rate decreased step by step from 2.0 to 1.2 A/cm² equivalent. The voltage data

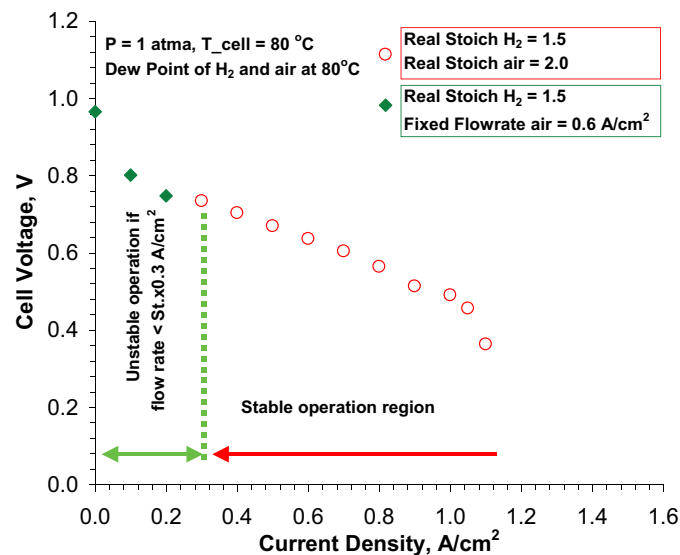


Figure 6. I - V polarization curve under real stoichiometry control: $\xi_a = 1.5$, $\xi_c = 2.0$ of real current density, and 1 atm.

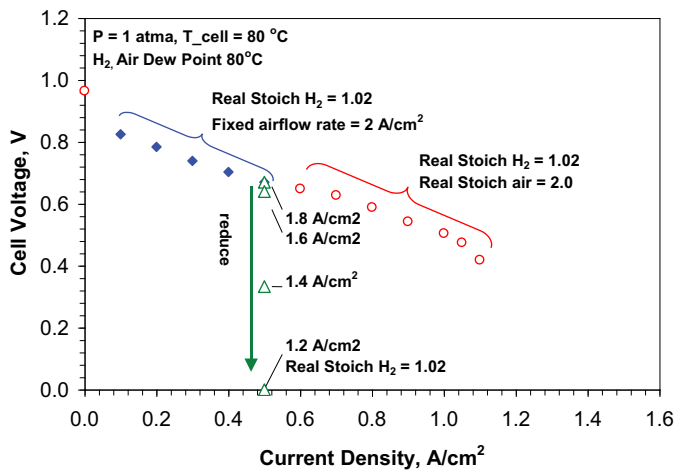


Figure 7. I - V polarization curve under real stoichiometry control: $\xi_a = 1.02$, $\xi_c = 2.0$ of real current density, and 1 atm. For the fixed airflow rate of 2 A/cm^2 , the stoichiometry is 2.0 at 1 A/cm^2 .

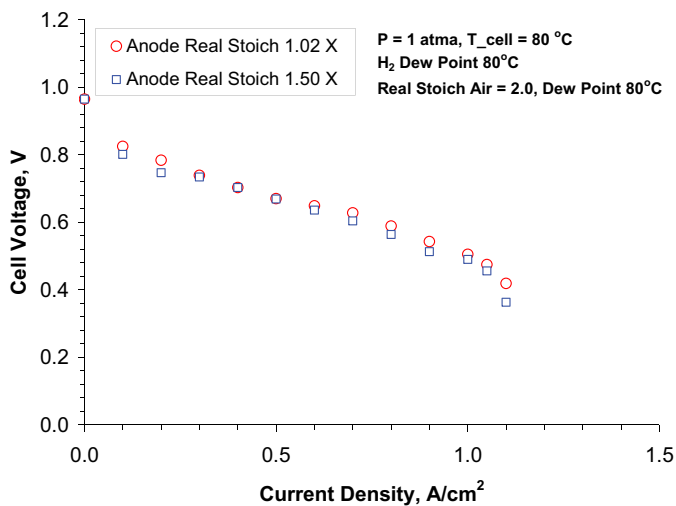


Figure 8. Comparison between normal (1.5) and ultra-low (1.02) real anode stoichiometry at 1 atm. Detailed test conditions could be found in Figures 6 and 7.

at different airflow rates are shown by the vertical array of dots in Figure 7. In the airflow range of 2.0–1.6 A/cm^2 eq., the cell was able to run stably all the time. If the airflow rate reduces to 1.4 A/cm^2 eq., which equals to a stoichiometry of ~ 3 @ 0.5 A/cm^2 , the cell voltage sets out to oscillate around 0.33 V. Reducing airflow rate to 1.2 A/cm^2 eq., the cell operation shut down immediately due to zero voltage. From this set of parametric investigation, we know that airflow stoichiometries shall be higher enough for the cell to run readily in the low-current regime.

Figure 8 provides performance comparison between tests with these two fuel stoichiometries at 1 atm. Both polarization plots are essentially the same, but the differences in threshold current densities. In high-current regime, polarization curve starts to deviate in both cases, indicative of the presence of mass depletion. Since hydrogen fed at an ultra-low stoichiometry does not affect the maximum current of the cell, mass depletion occurs at the cathode probably.

3.3. Effect of inlet humidification

3.3.1. Tests at 2 atm, $\xi_a/\xi_c = 1.5/2.0$ and drier air

All above tests were run under full humidification. To investigate the effect of inlet humidification on both cell performance and instability region, the following tests were conducted with relatively drier air feeding. In these tests, relative humidity of inlet air reduced to 50% relative humidity (RH) by setting the dew point of air bubbler at 63°C. With otherwise identical test parameters in Figure 1, the polarization performance is shown by dots in Figure 9. The typical performance was 0.782 V at 0.3 A/cm^2 , and 0.594 V at 1.0 A/cm^2 , respectively. In comparison with Figure 1, there is no sacrifice to cell performance, as air humidification reduces to 50%RH. The high tolerance to dry gases is attributed to the thin membrane used, which provides sufficient ionic conductance even under relatively dry air inlet conditions.

In this case, the threshold current of the instability regime was 0.3 A/cm^2 , the same as counterpart tests with fully humidified air feed. This consistency tells that the controlling factors for cell operation instability become less sensitive to air inlet humidification conditions.

Due to operational simplicity and/or low requirement for test hardware, PEFCs used to be tested under a fixed-flow-rate mode for fundamental researches, such as, electrochemical catalytic analysis and numerical simulation of cell/electrode reactions. The fixed-flow-rate mode means that gas flow rates were constant (e.g., 2 @ 1 A/cm^2) at any current densities. However, in this paper, all tests were conducted under a real-stoichiometry mode. It is desirable to compare results under these two different modes in the same work: the fixed-flow-rate mode and real-stoichiometry mode. For this reason, another set of fixed-flow-rate tests was included in Figure 9 too. The flow rates of hydrogen/air were constantly set at a stoichiometry of 1.5/2.0 @ 1 A/cm^2 , respectively, with other parameters unchanged. Thus the

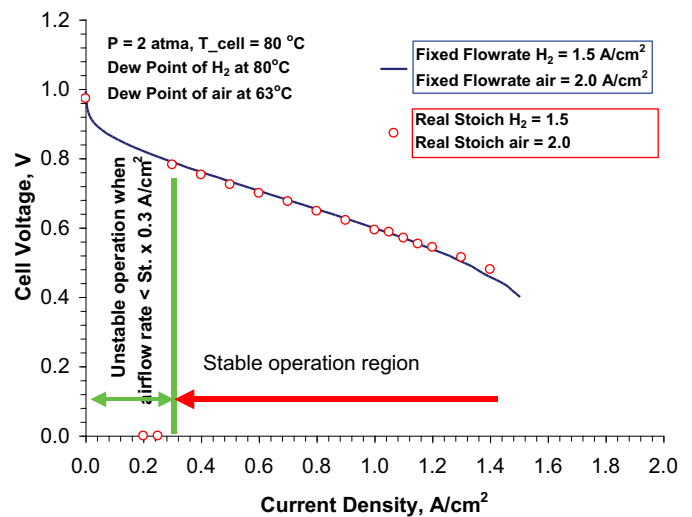


Figure 9. I - V polarization curve under real stoichiometry control: $\xi_a = 1.5$, $\xi_c = 2.0$ times real current density, 2 atm and drier air with 50% relative humidity. By comparison, I - V plot under the same test conditions except at fixed flow rates (H_2 /air) = 1.5/2.0 A/cm^2 is also included. For the fixed airflow rate of 2 A/cm^2 , the stoichiometry is 2.0 at 1 A/cm^2 .

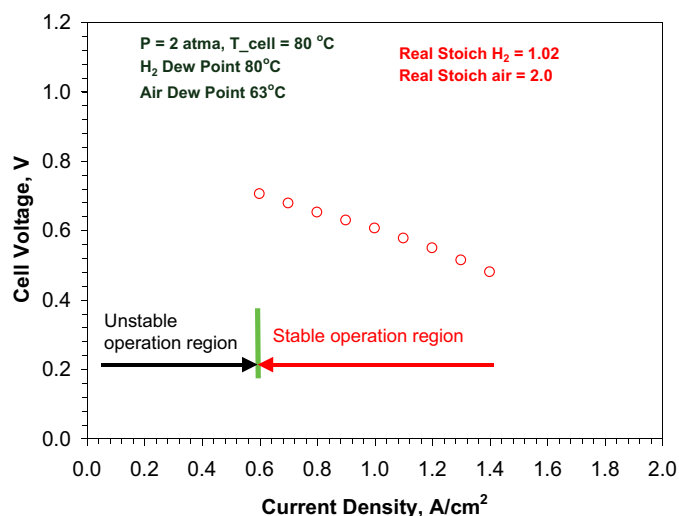


Figure 10. I–V polarization curve under real stoichiometry control: $\xi_a = 1.02$, $\xi_c = 2.0$ times real current density, 2 atm and drier air with 50% relative humidity.

actual stoichiometry appears much higher in the low current region. For instance, the actual stoichiometry was 15/20 (H_2 /air) when the current density was 0.1 A/cm^2 . Interestingly, the excess reactant gases did not promote cell performance at all in the low current regime, as shown in Figure 9. At high currents ($> 1 \text{ A/cm}^2$), the cell with a fixed-flow-rate showed a worse performance, because the actual stoichiometry reduced.

3.3.2. Test at 2 atm, $\xi_a/\xi_c = 1.02/2.0$ and drier air inlet (50% RH)

Reducing the hydrogen stoichiometry to 1.02, and remaining air inlet humidification at 50%RH, the cell performance is shown in Figure 10. Careful comparison between Figures 9 and Figures 10 reveals almost the same I–V performance for both cases with two stoichiometries at 2 atm. But, the threshold current appeared at 0.6 A/cm^2 at $\xi_a/\xi_c = 1.02/2.0$. It is interesting to see that reduced air humidification (50%RH at 2 atm) affects instability region in the same pattern as a reduced cell pressure (100%RH at 1 atm) does.

3.4. Discussion

One conclusion based on our experiments is that PEFCs can operate steadily with an ultra-low fuel stoichiometry (e.g., $\xi_a = 1.02$), and provide uncompromising power capability as it runs with normal fuel stoichiometry $\xi_{av} = 1.5$. The ultra-low fuel stoichiometry approach results in high fuel utilization, at the mean time, it does not lead to fuel depletion and thus degraded performance. This finding will be valuable in the strategy design of fuel feed and control systems in PEFCs.

All test results show the presence of operation instability in the low-current regime, when the cell runs under a real-stoichiometry-controlled mode. Increasing airflow rates manages to mitigate the occurrence of instable cell performance, while hydrogen is fed stoichiometrically ($\xi_a = 1.02$). So the possible cause of fuel

starvation can be excluded in the high fuel utilization strategy. In contrast, if increasing the fuel stoichiometry while keeping air stoichiometry $\xi_c = 2$ constant-, the cell was unable to function steadily in the low-current regime. It meant that the cell performance stability is intrinsically linked to cathode reaction.

The most possible cause for unstable performance is water flooding in the cathode, which is a common phenomenon with fully humidified reactant gases, water flooding used to occur at the cathode. Water droplet formation on GDLs and gas channels clogged by liquid water symbolize severe flooding cases (Ashrafi and Shams 2016; Benner, Mortazavi, and Santamaria 2018; Yang et al. 2004). Flooding takes place as a result of water accumulation exceeding water removal. This is likely to happen in tests typically in the low-current regime where airflow rate is very limited, and thus the removal of liquid water under shear drag force of the core airflow is ineffective. As a consequence, water accumulates and stations in channels, and finally clogs gas flow. Due to liquid water covering the active area, depletion of reactant gases at the active sites and thus lower local voltages are expected. This explains why performance instability occurs in the low-current region.

The other question is why reduced fuel stoichiometries extend the unstable region. For instance, as fuel stoichiometry ξ_a reduces from 1.5 to 1.02, the threshold current density of unstable regions increases from 0.3 A/cm^2 to 0.7 A/cm^2 in Figure 3. In those comparative experiments, airflow stoichiometry always remained identical, so the capability of water removal by airflow was the same. One can see easily that fuel stoichiometry indeed affect the span of operation instability regions that are mainly related to cathode reactions as discussed above.

In other words, changing fuel stoichiometry appears to alter humidification condition in the cathode. Fuel velocity at the outlet is very low at $\xi_a = 1.02$, water resides easily over a larger coverage of anode GDL surface, and thus the anode may experience flooding too. Even so, test results showed steady cell performance with H_2 fed stoichiometrically at $\xi_a = 1.02$. It could be attributed to the facile diffusion and electrochemical reaction of hydrogen, as well as its high concentration in the anode channel. It is because the gas pressure along the anode channel is almost constant in spite of the low fuel stoichiometry. Therefore anode flooding may have little effect on cell performance stability. Previous studies showed that the electro-osmotic water drag coefficient will increase by $\sim 30\%$, when the membrane is exposed to liquid water (Zawadzinski et al. 1995) instead of gas water vapor. Considering a very thin membrane used in the present study, the presence of accumulated liquid water in anode will accelerate its transport to the cathode via electro-osmosis. Thus it requires at more airflow to remove the extra portion of water from the anode to maintain operation. Simulation data in the companion paper help illustrate this mechanism in detail (Wang, Yang, and Wang 2021). A literature paper similarly indicated that the performances of individual cell and stack do not change with the increase in the anode gas stoichiometric ratio, but increase with the increase in the cathode gas stoichiometric ratio (Jang et al. 2008).

Performance instability is found to be specific to operational conditions, as a function of factors pertaining to flooding issue, such as flow field design, cell size or cell stack, temperature and flow rate, etc. These factors will change the span of operation instability regime; however, they probably will not get rid of its occurrence completely. Besides performance instability, non-uniformity in reactants' distribution and thus performance distribution over entire cell or stack is also expected (Stumper et al. 1998; Yang et al. 2005).

4. Conclusion

Ultrahigh fuel utilization strategy and its impact on cell performance and operation stability have been studied experimentally in this paper. The strategy directly employs a nearly unity stoichiometric flow for anode hydrogen gas, thus reduces complex hardware requirement. The study showed that when hydrogen real stoichiometry ξ_a reduced from 1.5 to 1.02, both test results showed identical cell performance (i.e., 1 A/cm² at 0.6 V and 2 atm). No loss in cell performance with $\xi_a = 1.02$ can be explained by hydrogen enrichment downstream in the anode flow field. Unstable operation regions symbolized by cell voltage fluctuation were observed in the low power regime for both fuel stoichiometries; however, the unstable region expanded from 0–0.3 A/cm² to 0–0.7 A/cm² as the real stoichiometry ξ_a reduced from 1.5 to 1.02. Parametric studies indicated that the operation instability was mainly due to low airflows rather than fuel starvation. The relationship between high-fuel utilization and greater airflow rates required for steady cell operation can be explained by an altered water management within the cell. Experimental results indicated that the cell could run steadily with no sign of performance loss under an ultra-low fuel stoichiometry. Numerical simulation aiming at this approach will be published in a companion paper.

ORCID

C.Y. Wang  <http://orcid.org/0000-0003-0650-0025>

References

- Ashrafi, M., and M. Shams. 2016. Effects of heterogeneous surface of gas diffusion layers on droplet transport in microchannels of PEM fuel cells. *International Journal of Hydrogen Energy* 41 (3):1974–89. doi:10.1016/j.ijhydene.2015.11.096.
- Benner, J., M. Mortazavi, and A. D. Santamaria (2018, November). Numerical simulation of droplet emergence and growth from gas diffusion layers (GDLs) in proton exchange membrane (PEM) fuel cell flow channels. ASME 2018 International Mechanical Engineering Congress and Exposition. Pittsburgh, Pennsylvania, USA: American Society of Mechanical Engineers Digital Collection.
- Berg, P., K. Promislow, J. St., P. J. Stumper, and B. Wetton. 2004. Water Management in PEM Fuel Cells. *Journal of the Electrochemical Society* 151:A341. doi:10.1149/1.1641033.
- Chakraborty, U. K. 2019. A new model for constant fuel utilization and constant fuel flow in fuel cells. *Applied Sciences* 9 (6):1066. doi:10.3390/app9061066.
- Du Plooy, D., J. Meyer, and S. von Solms (2018, April). Adaptive purging control of hydrogen fuel cells for high efficiency applications. 2018 International Conference on the Domestic Use of Energy (DUE) (1–6). Cape Town, South Africa: IEEE.
- Grimm, M., M. Hellmann, H. Kemmer, and S. Kabelac. 2020. Water management of PEM fuel cell systems based on the humidity distribution in the anode gas channels. *Fuel Cells* 20 (4):477–86. doi:10.1002/fuce.202000070.
- Ichikawa, Y., N. Oshima, Y. Tabuchi, and J. Keigo Ikezoe. 2014. Transient analysis of gas transport in anode channel of a polymer electrolyte membrane fuel cell with dead-ended anode under pressure swing operation. *Power Sources* 272:743–52. doi:10.1016/j.jpowsour.2014.09.023.
- Jang, J.-H., H.-C. Chiu, W.-M. Yan, and J. Wei-Lian Sun. 2008. Effects of operating conditions on the performances of individual cell and stack of PEM fuel cell. *Power Sources* 180:476–83. doi:10.1016/j.jpowsour.2008.02.001.
- Jiang, H., L. Xu, C. Fang, X. Zhao, Z. Hu, J. Li, and M. Ouyang. 2017. Experimental study on dual recirculation of polymer electrolyte membrane fuel cell. *International Journal of Hydrogen Energy* 42 (29):18551–59. doi:10.1016/j.ijhydene.2017.04.183.
- Manokaran, A., S. Pushpavanam, P. Sridhar, and S. Pitchumani. 2011. Experimental analysis of spatio-temporal behavior of anodic dead-end mode operated polymer electrolyte fuel cell. *Journal of Power Sources* 196 (23):9931–38. doi:10.1016/j.jpowsour.2011.06.103.
- O'hayre, R., S. W. Cha, W. Colella, and F. B. Prinz. 2016. *Fuel cell fundamentals*. John Wiley & Sons.
- Rabbani, A., and M. Rokni. 2013. Effect of nitrogen crossover on purging strategy in PEM fuel cell systems. *Applied Energy* 111:1061–70. doi:10.1016/j.apenergy.2013.06.057.
- Stumper, J., S. Campell, D. Wilkinson, M. Johnson, and M. Davis. 1998. In-situ methods for the determination of current distributions in PEM fuel cells. *Electrochimica acta* 43:3773. doi:10.1016/S0013-4686(98)00137-6.
- Toghyani, S., E. Afshari, and E. Baniasadi. 2019. A parametric comparison of three fuel recirculation system in the closed loop fuel supply system of PEM fuel cell. *International Journal of Hydrogen Energy* 44 (14):7518–30. doi:10.1016/j.ijhydene.2019.01.260.
- Toghyani, S., E. Baniasadi, and E. Afshari. 2018. Performance analysis and comparative study of an anodic recirculation system based on electrochemical pump in proton exchange membrane fuel cell. *International Journal of Hydrogen Energy* 43 (42):19691–703. doi:10.1016/j.ijhydene.2018.08.194.
- Voss, H. H., D. P. Wilkinson, P. G. Pickup, M. C. Johnson, and V. Basura. 1995. Anode water removal: A water management and diagnostic technique for solid polymer fuel cells. *Electrochimica Acta* 40 (3):321–28. doi:10.1016/0013-4686(94)00266-4.
- Wang, Y., S. Basu, and J. Chao-Yang Wang. 2008. Modeling two-phase flow in PEM fuel cell channels. *Power Sources* 179:603–17. doi:10.1016/j.jpowsour.2008.01.047.
- Wang, Y., X. G. Yang, and C. Y. Wang. 2021. *International Journal of Green Energy in press*, 2021.
- Xing, L., S. Du, R. Chen, M. Mamlouk, and K. Scott. 2016. Anode partial flooding modelling of proton exchange membrane fuel cells: Model development and validation. *Energy* 96:80–95. doi:10.1016/j.energy.2015.12.048.
- Yang, X. G., N. Burke, C. Y. Wang, K. Tajiri, and K. Shinohara. 2005. Simultaneous measurements of species and current distributions in a PEFC under low-humidity operation. *Journal of the Electrochemical Society* 152 (4):A759. doi:10.1149/1.1864492.
- Yang, X. G., F. Y. Zhang, A. L. Lubawy, and C. Y. Wang. 2004. Visualization of liquid water transport in a PEFC. *Electrochem. Solid-State Letters* 7:A408. doi:10.1149/1.1803051.
- Zawadzinski, T. A., J. Davey, J. Valerio, and S. Gottesfeld. 1995. The water content dependence of electro-osmotic drag in proton-conducting polymer electrolytes. *Electrochimica acta* 40:297. doi:10.1016/0013-4686(94)00277-8.